

1. Solar Wind – LISM Interaction.

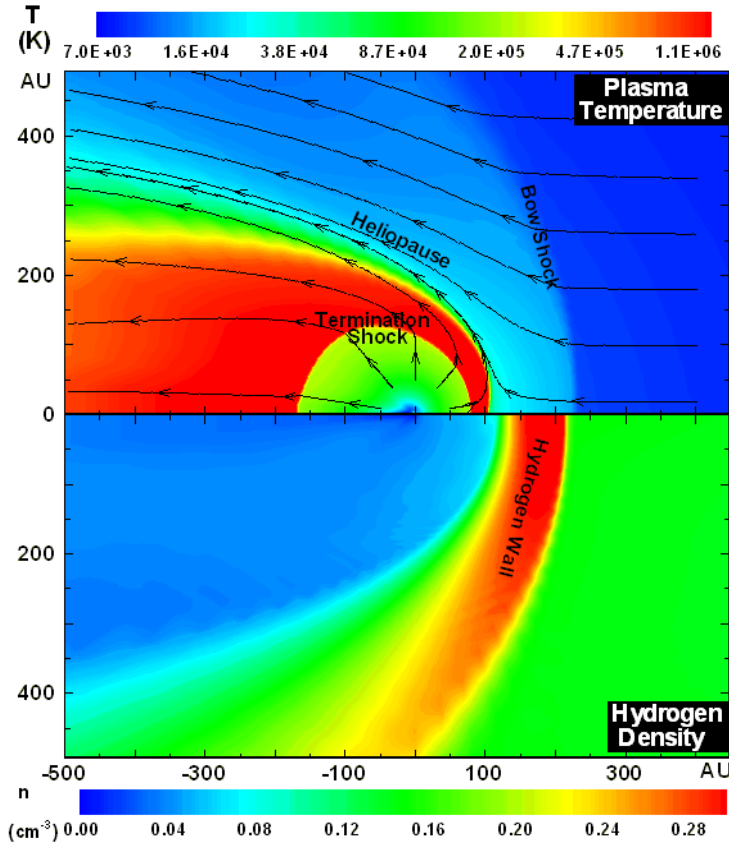


Figure 1: A computational model of the large-scale heliosphere and the local interstellar medium showing the plasma and the neutral hydrogen structure.

We have been instrumental in elucidating the physics of the solar wind – Local Interstellar Medium (LISM) interaction using a combination of sophisticated numerical codes, analytical modeling and testing against observations (some of which, such as Lyman-alpha absorption measurements, have not hitherto been part of the traditional observational tools used by space physicists). Our work predicted the existence of the hydrogen wall, a region of heated, compressed neutral interstellar hydrogen adjacent to and beyond the heliopause. The fortuitous discovery a few years later by Jeff Linsky and Brian Wood of unexplained Lyman-alpha absorption in Hubble GHRS spectra in the upstream direction was interpreted as possible evidence for the existence of the hydrogen wall, and we showed that the Ly-alpha absorption measurements could be fitted to spectra derived from global heliospheric models, which included the physics of the interaction between plasma and neutral interstellar hydrogen. Our models have become increasingly sophisticated as we continue to incorporate more physical processes.

This work is of great interest computationally because it represents a new approach to computing. Since our models allow us to compute the expected flux of energetic neutral atoms at 1 AU created in the boundaries of the solar wind, our work is of great interest and importance to the upcoming IBEX mission.

2. Turbulence. Understanding turbulence in the solar wind and interstellar medium provides insight into the transport and partitioning of energy in these environments, into the scattering and transport of energetic particles such as cosmic rays, the energization of particles at shock waves or large-scale solar coronal magnetic fields, the heating of plasma, and so forth. We have developed the theory of *nearly incompressible MHD* (NI MHD), motivated by an earlier suggestion by David Montgomery to explain the observed universal Kolmogorov-like power law spectrum of (electron) density fluctuations. This work showed explicitly and constructively the connection between compressible and incompressible fluids, including MHD, and was thus of immediate importance to our understanding of solar wind fluctuations, which appear to exhibit characteristics of both descriptions at different times. This work has led now to a new paradigm for solar wind turbulence, *viz.*, anisotropic turbulence comprised of a superposition of 2D

turbulence and slab turbulence, with the power in the respective fluctuations approximately in the ratio of 80% to 20%. Observations appear to confirm not only the superposition model but the approximate ratio as well. Such a result is very different from our earlier ideas about turbulence in the solar wind which assumed either isotropic or slab descriptions of solar wind turbulence.

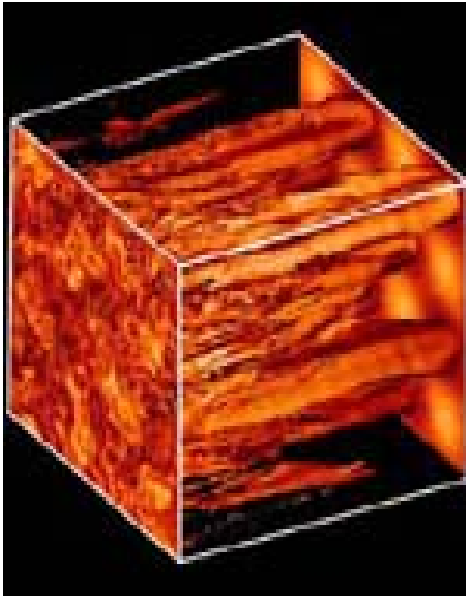


Figure 2: The evolution of flux tubes in the presence of an admixture of 2D turbulence and slab turbulence. This illustrates the “wandering” of magnetic field lines – an explanation for the large diffusive movement of energetic particles in directions perpendicular to the mean or ambient interplanetary magnetic field.

A second area in which we have made contribution to our understanding of turbulence in the solar wind is in the radial and temporal evolution of the energy density in solar wind magnetic fluctuations. The theory exhibits very close agreement with Voyager and Pioneer observations to 80 AU, and is shown in Figure 3 out to 40 AU. This work reconciles the turbulence perspective of the solar wind (dissipative heating, spectra, etc.) with the observed radial decay in fluctuation energy, providing a tractable paradigm for the dynamical transport of MHD turbulence in the inhomogeneous solar wind.

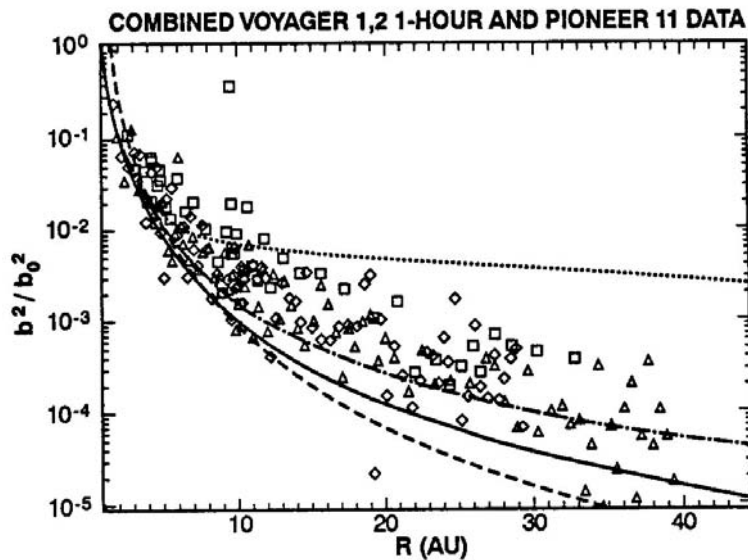


Figure 3: Plot of the energy density in magnetic field fluctuations showing a set of theoretically derived curves overplotted with Voyager and Pioneer spacecraft data.

3. Solar energetic particle events and Space Weather. We have developed physics based models that describes gradual solar energetic particle and energetic storm particle events. It had been thought that interplanetary shock waves were responsible for accelerating the solar wind ions that were commonly seen as large enhancements in the flux of energetic particles measured by spacecraft. The shock waves are typically driven by coronal mass ejections (CMEs). We have developed a numerical model of the shock propagation and tied this into a time-dependent particle acceleration model. This approach utilizes a sophisticated transport model based on a time-dependent implementation of a Monte-Carlo algorithm and models the wave-particle interaction using a quasi-linear approach (for quasi-parallel shocks). Our model allows us to predict time intensity particle profiles, particle spectra, particle anisotropies, etc., at 1 AU and throughout the heliosphere.

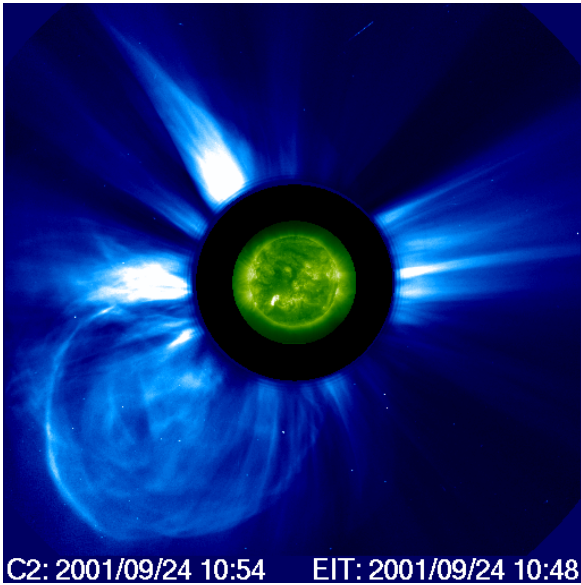


Figure 4: A coronal mass ejection observed by EIT

4. Scientific computation research interests Many problems in the physical sciences are characterized by the presence of multiple and often disparate length or time scales. To address the multiplicity of scales often requires the use of different physical descriptions or models, each appropriate to the regime of interest. Thus many computationally challenging problems in space physics and astrophysics require that hitherto distinct or separate algorithms and computational methods be fused. The fusion of distinct algorithms and techniques to challenging computational problems in space physics and astrophysics is a major component of our research.

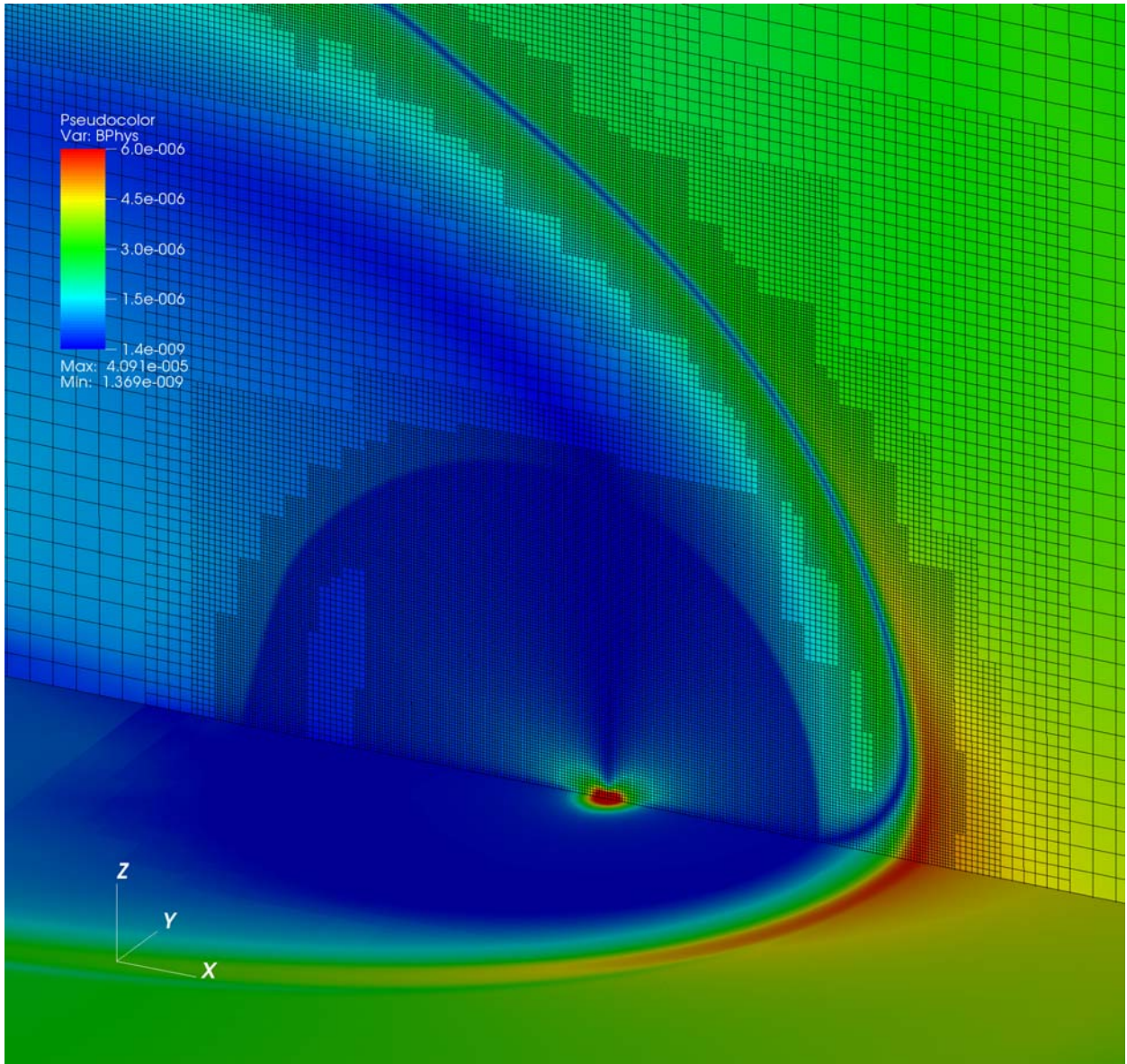


Figure 5: The distribution of magnetic field strength in the meridional ($z0x$) and ecliptic ($x0y$) planes and the computational grid adapted to discontinuities in the solution of the solar wind – local interstellar medium interaction problem. The computational adaptive mesh has four additional levels. Base resolution: $80 \times 100 \times 100$. Effective resolution: $1280 \times 1600 \times 1600$. Finest grid size: 1.25AU